A Time-Domain High-Order Spectral Finite Element for the Simulation of Symmetric and Anti-Symmetric Guided Waves in Laminated Composite Strips with Active Piezoelectric Sensors

Christoforos Rekatsinas, Christos Nastos, Theodosis Theodosiou, Dimitris Saravanos

7th European Workshop on Structural Health Monitoring
July 8-11, 2014. La Cité, Nantes, France

A TIME-DOMAIN HIGH-ORDER SPECTRAL FINITE ELEMENT FOR THE SIMULATION OF SYMMETRIC AND ANTI-SYMMETRIC GUIDED WAVES IN LAMINATED COMPOSITE STRIPS WITH ACTIVE PIEZOELECTRIC SENSORS

Christoforos Rekatsinas[1], Christos Nastos[1], Theodosis Theodosiou[2], Dimitris Saravanos[3]

Dept. of Mechanical Engineering & Aeronautics, University of Patras, GR-26500, Rion-Patras, Greece

saravanos@mech.upatras.gr

ABSTRACT

A new time domain spectral finite element is developed for improving the efficiency of numerical simulations of guided waves in laminated composite strips. The finite element relies on a new generalized laminate mechanics model formulated to represent symmetric and anti-symmetric Lamb waves. The laminate mechanics incorporate third-order polynomial terms for the approximation of axial and transverse displacement fields through the thickness, and consider the displacements of the upper and lower surfaces as degrees of freedom. Based on the resultant governing equations of the laminate section, a new finite element with 8 nodal degrees of freedom is formulated, with its nodes collocated with Gauss-Lobatto-Legendre integration points. Stiffness and mass matrices are assembled and the transient response is predicted with explicit central differences time integration. The transient response of an orthotropic composite strip exited by a 5-count Gaussian pulse is investigated. Results are validated against a semi-analytical solution Numerical results exhibit substantial improvement in the convergence and accuracy of the introduced element regarding the prediction of symmetric and anti-symmetric wave propagation.

KEYWORDS : *Time Domain Spectral Elements, Transient Response, Ultrasonic Lamb Waves*

INTRODUCTION

The expansion of Lamb wave SHM methods to composite materials and structures brings new challenges due to the material and damage complexity. Thus, the design of effective SHM methods in composites requires the development of innovative analytical and numerical tools for the simulation and analysis of wave propagation in healthy and damaged composites. Numerous approaches, including the Finite Difference Method [***1***] and the classical Finite Element Analysis (FEA) [***2***], have been proposed and successfully applied on the simulation of generated waves and the prediction of the transient response in the time and space domain. However, when high frequencies and wavenumbers are involved, traditional methods require very fine spatial and temporal discretization to ensure numerical stability; apart from the excessive computational load, such a fine discretization can exceed the Niquist criterion limit and invalidate the analysis [***3***]. On the other hand, the use of the Boundary Elements [***4***] or Spectral Frequency Finite Elements [***5***] may reduce the size of spatial discretization, but their implementation in the frequency domain requires special treatment for application on structures of finite dimensions [***6***]. A more advanced FEA-based approach targeting simulations of guided wave propagation is the Time Domain Spectral Finite Element (TDSFE)

[1] Ph.D student
[2] Post Doctoral Fellow
[3] Professor; Corresponding author. Tel +30-2610-969437, email: saravanos@mech.upatras.gr

Method, introduced by Patera in the mid of 80's [*7*]. This employs features of classical FEA, like local approximation and variational formulation, but uses high-order polynomial shape functions and integration points collocated with the element nodes; the latter results in consistent diagonal mass matrices. The TSSFE method can be combined with well-known explicit time integration schemes and has proved to be more efficient and accurate than traditional FEs in the simulation of wave propagation in 1-, 2- [*8*] [*9*] and 3D structures [*10*].
Most reported works on TDSFEs involve continuous 2D and 3D finite element formulations for the simulation of wave propagation in strips and plates respectively, which require s lot of nodes and DOFs through the thickness of the structure. This work, on the other hand, describes the development of a TDSFE for composite strips based on a generalized high-order laminate theory [*11*] which is optimized for the efficient approximation of the first symmetric (S_0) and anti-symmetric (A_0) modes. The laminate model is combined with the TDSFE formulation along the axial direction to improve the accuracy and numerically efficiency of wave scattering prediction through isotropic and laminated strips.
In order to make this paper self-consistent, elements of the High-Order Laminate Theory (HOLT) are also presented. The developed is employed towards the prediction of S_0 and A_0 modes in composite strips. The accuracy and convergence of the developed TDSFE is validated against a semi-analytical solution, a First Order Shear Element and a traditional 2D plain strain FE.

1 THEORETICAL BACKGROUND

1.1. KINEMATIC ASSUMPTIONS

Lamb waves are a special type of ultrasonic waves that propagate between two parallel stress-free surfaces. The Lamb wave equation has been derived based on the assumption of straight-crested waves. Depending on the excitation frequency and material properties, numerous fundamental vibration modes may be excited; these can be categorized based on the symmetry of the displacement fields with respect to the mid-plane, thus, giving rise to symmetric (S_i) and anti-symmetric (A_i) modes, $i \in \mathbb{N}$.
The longitudinal (u) and transverse (w) displacement fields of the fundamental symmetric and anti-symmetric wave modes for a strip are derived from the Rayleigh-Lamb equation as sums of sine and cosine terms [*12*]:

$$\begin{aligned} S_i: &\quad u(z) \simeq A\cos(az) + B\cos(bz), \quad w(z) \simeq C\sin(az) + D\sin(bz) \\ A_i: &\quad u(z) \simeq A\sin(az) + B\sin(bz), \quad w(z) \simeq C\cos(az) + D\cos(bz) \end{aligned} \tag{1}$$

where a, b are the thickness wavenumbers and h is the plate thickness. Considering applications of practical significance involving the S_0 and A_0 modes. Then the sine and cosine terms can be sufficiently approximated using the first two terms of the Taylor expansion series:

$$\cos(az) \simeq 1 - \frac{1}{2}(az)^2, \quad \sin(az) \simeq az - \frac{1}{6}(az)^3 \tag{2}$$

In order to obtain a better approximation of the displacement fields and the boundary conditions the constant and linear terms in the previous equations can be recast as:

$$u(x,z,t) = u^1(x,t)\cdot\Psi^1(\zeta) + u^2(x,t)\cdot\Psi^2(\zeta) - \gamma_x(x,t)\cdot\frac{\zeta^2-1}{2} - \delta_x(x,t)\cdot\zeta\cdot\frac{\zeta^2-1}{6} \tag{3}$$

$$w(x,z,t) = w^1(x,t)\cdot\Psi^1(\zeta) + w^2(x,t)\cdot\Psi^2(\zeta) - \gamma_z(x,t)\cdot\frac{\zeta^2-1}{2} - \delta_z(x,t)\cdot\zeta\cdot\frac{\zeta^2-1}{6} \tag{4}$$

The coefficients u^1, w^1, u^2, w^2 denote the displacements at the bottom and top surfaces respectively [*13*] and can be thought as the effective extension and rotation of the strip; $\zeta = \frac{2z}{h}$ and $\Psi(\zeta)$ are linear interpolation functions through the layer thickness and they are equal to

$$\Psi_1(\zeta)=\frac{1-\zeta}{2},\quad \Psi_2(\zeta)=\frac{1+\zeta}{2} \tag{5}$$

Using extended vector notation, the assumed displacement field can be expressed as:

$$\mathbf{u}(x,z,t)=\left[\mathbf{Z_u}\right]\mathbf{U_L}(\mathbf{x},\mathbf{t}) \tag{6}$$

where $\mathbf{u}=[u,w]^T$ and $\mathbf{U}_L=\left[u^1,u^2,w^1,w^1,\gamma_x,\gamma_z,\delta_x,\delta_z\right]^T$ represent the generalized laminate degrees of freedom.

1.2. STRAIN-DISPLACEMENT RELATION

The relation between the displacements and the axial (ε_1), transverse (ε_3) and shear (ε_5) strain of each ply can be derived from Eqs. (3)-(4):

$$\varepsilon_1=\varepsilon_x=\frac{u^1_{,x}+u^2_{,x}}{2}+\frac{\gamma_{x,x}}{2}+\left(\frac{u^2_{,x}-u^1_{,x}}{2}+\frac{\delta_{x,x}}{6}\right)\cdot\zeta_n-\frac{\gamma_{x,x}}{2}\cdot\zeta_n{}^2-\frac{\delta_{x,x}}{6}\cdot\zeta_n{}^3 \tag{7}$$

$$\varepsilon_3=\varepsilon_z=\frac{w^2-w^1}{h}+\frac{\delta_z}{3h}-\frac{2\gamma_z}{h}\zeta_n-\frac{\delta_z}{h}\zeta_n{}^2 \tag{8}$$

$$\begin{aligned}\varepsilon_5=\varepsilon_{xz}\quad&=\frac{u^2-u^1}{h}+\frac{w^1_{,x}+w^2_{,x}}{2}+\frac{\gamma_{z,x}}{2}+\frac{\delta_x}{3h}+\\&+\left(\frac{w^2_{,x}-w^1_{,x}}{2}-\frac{2}{h}\gamma_\chi+\frac{1}{6}\delta_{z,x}\right)\cdot\zeta_n-\left(\frac{\gamma_{z,x}}{2}+\frac{\delta_x}{h}\right)\cdot\zeta_n{}^2-\frac{\delta_{z,x}}{6}\cdot\zeta_n{}^3\end{aligned} \tag{9}$$

The terms $\gamma_{x,x},\delta_{x,x},\gamma_{z,x},\delta_{z,x}$ are first order derivatives of the hyper-rotation coefficients in Eqs. (3)-(4) . The normal transverse strain in Eq. (8) is one of the novelties introduced in this paper as it allows for quadratic and cubic approximations through the thickness of the laminate.

Employing again extended vector notation, strain expression in Eqs. (7)-(9) can be compacted to $\boldsymbol{\varepsilon}=\left[\varepsilon_1,\varepsilon_3,\varepsilon_5\right]^T$, and in accordance to Eq. (6):

$$\boldsymbol{\varepsilon}=\left[\mathbf{Z}_{\boldsymbol{\varepsilon}}\right]\cdot\boldsymbol{\varepsilon}_\mathbf{L} \tag{10}$$

In the previous relation $\boldsymbol{\varepsilon}_\mathbf{L}=\left[\varepsilon_{x0},\kappa_{x1},\kappa_{x2},\kappa_{x3},\varepsilon_{z0},\kappa_{z1},\kappa_{z2},\varepsilon_{xz0},\kappa_{xz1},\kappa_{xz2},\kappa_{xz3}\right]^T$ is the generalized strain vector, where $\varepsilon_0,\kappa_1,\kappa_2,\kappa_3$ represent the constant, linear, quadratic and cubic term coefficients in Eqs. (7)-(9). Finally, the $\left[\mathbf{Z}_{\boldsymbol{\varepsilon}}\right]$ matrix appearing in Eq. (10) is expressed as:

$$\left[\mathbf{Z}_{\boldsymbol{\varepsilon}}\right]=\begin{bmatrix}1&\zeta&\zeta^2&\zeta^3&0&0&0&0&0&0&0\\0&0&0&0&1&\zeta&\zeta^2&0&0&0&0\\0&0&0&0&0&0&0&1&\zeta&\zeta^2&\zeta^3\end{bmatrix} \tag{11}$$

1.3. GENERALIZED EQUATIONS OF EQUILIBRIUM AND LAMINATE MATRICES

According to the principal of virtual work [*14*] the strain energy variation of a laminate can be expressed in terms of the work of inertial forces and tractions. Based on this, the equilibrium equations are expressed as:

$$\int_0^L\left\{\int_{-\frac{h}{2}}^{\frac{h}{2}}\delta\boldsymbol{\varepsilon}^T\cdot\left[\mathbf{Q_c}\right]\cdot\boldsymbol{\varepsilon}dz+\int_{-\frac{h}{2}}^{\frac{h}{2}}\delta u\cdot\left(-\rho\ddot{u}\right)+\delta w\cdot\left(-\rho\ddot{w}\right)dz+\left[\delta\bar{u}\cdot\tau_{xz}+\delta\bar{w}\cdot\tau_z\right]_{-\frac{h}{2}}^{\frac{h}{2}}\right\}dx=0 \tag{12}$$

where $\left[\mathbf{Q_c}\right]$ is the stiffness matrix of a composite ply with arbitrary rotation and ρ is the mass density. Incorporation of Eq. (11) into (12) leads to

$$\delta V_L = \int_0^L \left\{ \frac{h}{2} \int_{-1}^{1} \delta \boldsymbol{\varepsilon}_L^T \cdot \left[\mathbf{Z}_{\boldsymbol{\varepsilon}}\right]^T \cdot \left[\mathbf{Q}_{\mathbf{c}}\right] \cdot \left[\mathbf{Z}_{\boldsymbol{\varepsilon}}\right] \cdot \boldsymbol{\varepsilon}_L d\zeta \right\} dx = \int_0^L \delta \boldsymbol{\varepsilon}_L^T \cdot \left[\mathbf{K}_{\mathbf{L}}\right] \cdot \boldsymbol{\varepsilon}_L dx \tag{13}$$

where $\left[\mathbf{K}_{\mathbf{L}}\right]$ is the generalized stiffness matrix of the laminate and is equal to:

$$\left[\mathbf{K}_{\mathbf{L}}\right] = \begin{bmatrix} \left[\mathbf{K}_{\mathbf{L11}}\right] & \left[\mathbf{K}_{\mathbf{L13}}\right] & 0 \\ \left[\mathbf{K}_{\mathbf{L13}}\right]^T & \left[\mathbf{K}_{\mathbf{L33}}\right] & 0 \\ 0 & 0 & \left[\mathbf{K}_{\mathbf{L}55}\right] \end{bmatrix} \tag{14}$$

The constituent submatrices can be further expanded as:

$$\left[\mathbf{K}_{\mathbf{L11}}\right] = \begin{bmatrix} A_{11} & B_{11} & D_{11} & E_{11} \\ B_{11} & D_{11} & E_{11} & F_{11} \\ D_{11} & E_{11} & F_{11} & G_{11} \\ E_{11} & F_{11} & G_{11} & H_{11} \end{bmatrix} \quad \left[\mathbf{K}_{\mathbf{L13}}\right] = \begin{bmatrix} A_{13} & B_{13} & D_{13} \\ B_{13} & D_{13} & E_{13} \\ D_{13} & E_{13} & F_{13} \\ E_{13} & F_{13} & G_{13} \end{bmatrix}$$

$$\left[\mathbf{K}_{\mathbf{L33}}\right] = \begin{bmatrix} A_{33} & B_{33} & D_{33} \\ B_{33} & D_{33} & E_{33} \\ D_{33} & E_{33} & F_{33} \end{bmatrix} \quad \left[\mathbf{K}_{\mathbf{L55}}\right] = \begin{bmatrix} A_{55} & B_{55} & D_{55} & E_{55} \\ B_{55} & D_{55} & E_{55} & F_{55} \\ D_{55} & E_{55} & F_{55} & G_{55} \\ E_{55} & F_{55} & G_{55} & H_{55} \end{bmatrix} \tag{15}$$

The subscripts "11", "33" and "55" denote the axial, transverse and shear stiffness terms, respectively. The subscript "13" indicates coupling between axial and transverse stiffness. The generalized laminate stiffness coefficients of a laminate are calculated form:

$$\left\langle A_{ij}, B_{ij}, D_{ij}, E_{ij}, F_{ij}, G_{ij}, H_{ij} \right\rangle = \frac{h}{2} \sum_{k=1}^{N_p} \int_{\zeta_\kappa}^{\zeta_{\kappa+1}} Q_{cij} \left\langle 1, \zeta, \zeta^2, \zeta^3, \zeta^4, \zeta^5, \zeta^6 \right\rangle d\zeta \tag{16}$$

where, N_p is the number of plies and $\zeta_\kappa, \zeta_{\kappa+1}$ are the normalized thickness coordinates at the bottom and top face of each ply. The inertia body force term in Eq. (12) becomes:

$$\delta T_L = \int_0^L \left\{ \frac{h}{2} \int_{-1}^{1} \delta \mathbf{U}_L^T \cdot \left[\mathbf{Z}_{\mathbf{u}}\right]^T \cdot \left[diag(\rho) \right] \cdot \left[\mathbf{Z}_{\mathbf{u}}\right] \cdot \mathbf{U}_L \, d\zeta \right\} dx = \int_0^L \delta \mathbf{U}_L^T \cdot \left[\boldsymbol{\rho}_{\mathbf{L}}\right] \cdot \mathbf{U}_L dx \tag{17}$$

where, $[\rho_L]$ is the generalized laminated density matrix.

2 TIME DOMAIN SPECTRAL FINITE ELEMENT

The generalized equations presented in the previous section are used as a foundation for developing a beam finite element with C_0 Lagrange shape functions. Exploitation of high order Lagrangian Polynomial shape functions ensures the efficient spatial approximation of high wavenumbers in the plane of the beam. The nodes of the proposed element are located at Gauss-Lobatto-Legendre (GLL) integration points provided as solutions of $\left(1-\xi_i^2\right) \cdot P_{p,\xi}\left(\xi_i\right) = 0$, where $-1 \le \xi \le 1$ is the local coordinate of the element. Collocation of nodes with GLL integration points leads to diagonal or near diagonal mass matrices, which boost explicit time integration speed. Moreover, the uneven distribution of nodes near the ends of the element, yields uniform variation of shape functions along the element and eliminates undesired oscillations near the ends -the well- known Runge Phenomenon [*15*].

2.1. STIFFNESS AND MASS MATRICES

The element matrices of the proposed element are obtained from Eq.(12), following the same approach as in classical FEA. The elemental stiffness is, therefore, expressed as:

$$\left[\mathbf{K_e^{ij}}\right]=\frac{L_e}{2}\int_{-1}^{1}\left[\mathbf{R^i}\right]^T\cdot\left[\mathbf{K_L}\right]\cdot\left[\mathbf{R^j}\right]d\xi \tag{18}$$

In the same sense, the elemental mass matrix is:

$$\left[\mathbf{M_e^{ij}}\right]=\frac{L_e}{2}\int_{-1}^{1}\left[\mathbf{N^i}\right]^T\cdot\left[\boldsymbol{\rho}_\mathbf{L}\right]\cdot\left[\mathbf{N^j}\right]d\xi \tag{19}$$

In the previous relations $\left[\mathbf{R^i}\right],\left[\mathbf{N^i}\right]$ denote the strain and displacement shape function of the i[th] node respectively.

2.2. TIME INTEGRATION

Substitution of the elemental stiffness and mass matrices into the equation of motion leads to the discretized damped equations of motion:

$$[\mathbf{M}]\cdot\ddot{\mathbf{U}}(t)+[\mathbf{C}]\cdot\dot{\mathbf{U}}(t)+[\mathbf{K}]\cdot\mathbf{U}(t)=\mathbf{F}(t) \tag{20}$$

where [**M**] and [**K**] are the global mass and stiffness matrices respectively, [**C**] is a proportional damping matrix. The previous system of equations is solved using the central differences explicit integration scheme:

$$\left(\frac{1}{\Delta t^2}[\mathbf{M}]+\frac{1}{2\Delta t}[\mathbf{C}]\right)\cdot\mathbf{U}(t+\Delta t)=\mathbf{F}(t)-\left([\mathbf{K}]-\frac{2}{\Delta t^2}[\mathbf{M}]\right)\cdot\mathbf{U}(t)-\left(\frac{1}{\Delta t^2}[\mathbf{M}]-\frac{1}{2\Delta t}[\mathbf{C}]\right)\cdot\mathbf{U}(t-\Delta t) \tag{21}$$

with respect to $\mathbf{U}(t+\Delta t)$ at every time step. It has to be noted that Eq. (21) requires inversion only for the mass matrix, which is diagonal or nearly diagonal. Thus, solution of Eq. (21) is expected to be significantly higher than traditional FEA.

3 NUMERICAL RESULTS

The capability of the developed HOL-TDSFE to predict guided wave propagation, was evaluated on isotropic and orthotropic composite strips. As previously the strip was modelled with a uniform mesh of 40 9-node elements.

In this section, the introduced TDSFE is employed for the prediction of symmetric and anti-symmetric guided waves on a cross-ply $[0_2/90_2]_S$ Carbon/Epoxy strip. The material properties and specimen geometry are listed in Table 1. The left end of all strips (x=0) was simply supported and symmetry conditions were applied, while the other end remained free. Three types of loads are applied: a pair of transverse symmetric or anti-symmetric concentrated forces (F_z) at x = 0 to excite symmetric and antisymetric wave modes; and a shear surface traction τ_{xz}, [***16***], over a finite length L_a, which is equal to the 1/4 of the wavelength obtained by the dispersion curves of the tuned mode, to represent the induced stress by a piezoceramic actuator [***17***].

Table 1 Material Properties and Specimen Geometry

Ply Properties	
E1 (GPa)	127.0
E3 (GPa)	7.9
G13(GPa)	3.4
ν_{13}	0.275
ρ *(kg m^{-3})*	1578
Specimen Geometry	
Length (m)	1.5
Width (m)	1
Thickness (m)	0.002

The time variation of the forces amplitude forms a Hanning window time packet with 5 sinusoidal pulses of 0.5N maximum amplitude. The required time step for the time integration was set to the 1/5 of the period corresponding to the maximum natural frequency. Results obtained using the introduced TDSFE were validated against a semi-analytical solution that combines an exact analytical solution along the strip axis and a layerwise laminate theory through the thickness [***18***]. In order to quantify the superiority of the developed High-Order Laminate Theory (HOLT), its predictions are also compared to a model composed of 9-node TDSFEs based on a simpler Linear Laminate Theory model (LLT) which assumes only linear displacement fields through the thickness, by neglecting $\gamma_x,\gamma_z,\delta_x,\delta_z$. Figure 1 shows the predicted displacements for the cases of symmetric and anti- symmetric force pairs at 100 kHz, and quantifies the accuracy of the developed TDSFE for this highly inhomogeneous cross-ply laminate.

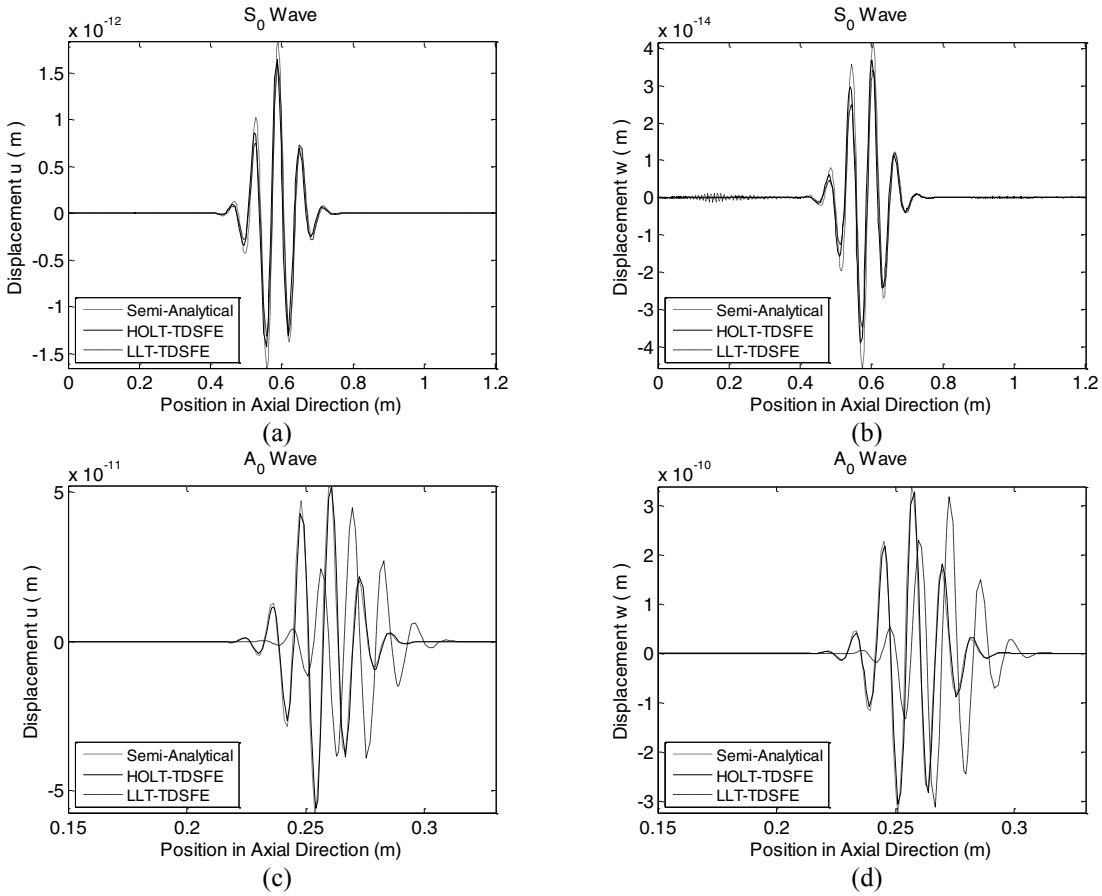

Figure 1 : Predicted axial and transverse wave displacements at the bottom surface of a $[0_2/90_2]_S$ CFRP Strip at t=0.00012 secs. a) and b) Symmetric force excitation; c) and d) Antisymmetric force excitation

In order to demonstrate the superiority of the developed beam element, its predictions are also compared to predictions of a TDSFE beam element employing Linear Laminate Theory (LLT). The through-thickness predictions for the cross-ply CFRP are shown in Figure 2.

Apparently, the greater accuracy of the introduced model is attributed to the inclusion of the high-order terms in Eqs. (3)-(4).

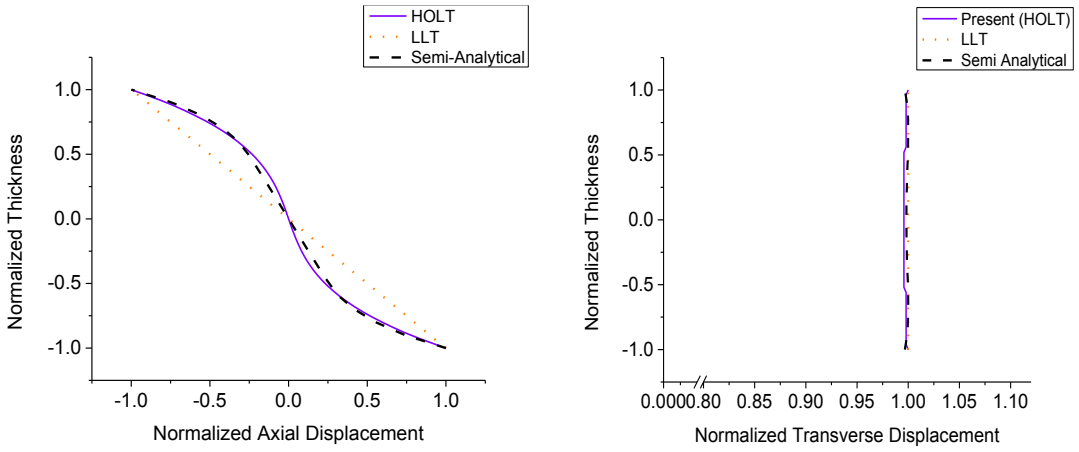

(a)

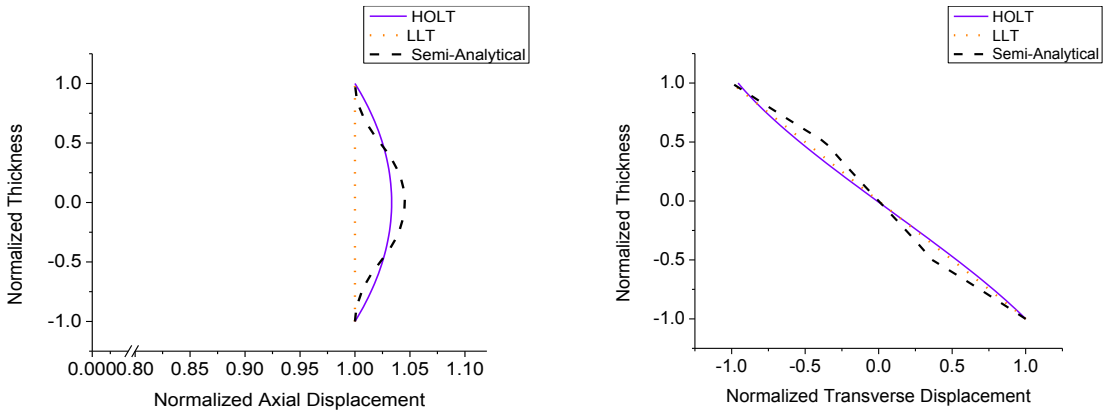

(b)

Figure 2 : Prediction of the displacement fields through the thickness of the $[0_2/90_2]_S$ CFRP strip. (a) Anti-Symmetric Loading; (b) Symmetric Loading.

Finally Figure 3 show the predicted wave response when the strip is excited by a shear traction stress applied at the upper surface. In closing, all predicted results support the fact that the proposed beam element can provide accurate results for the fundamental symmetric and antisymmetric guided waves of the examined laminate configurations.

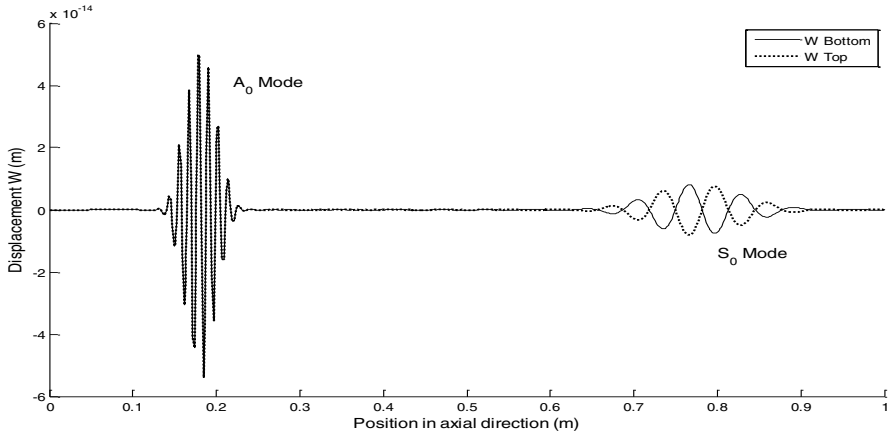

Figure 3 : Predicted wave propagation in $[0_2/90_2]_S$ CFRP Strip subject to surface shear traction due to piezoceramic actuator of length L_a.

SUMMARY

A new time domain explicit spectral beam element has been developed for the efficient analysis of guided waves in composite laminated strips. The introduced spectral element employs a high order lamination theory in order to accurately simulate symmetric and anti- symmetric Lamb wave propagation.

The accuracy, capability and effectiveness of the laminate theory and new finite element was demonstrated on Aluminum and Carbon/Epoxy unidirectional and cross-ply strips. Results are validated against a semi-analytical solution and are found to be in excellent agreement. The TDSFE can provide accurate predictions of the fundamental Ao and So guided waves in terms of amplitude, group velocity and dispersion. It can also capture nonlinear displacement fields through-the-thickness.

ACKNOWLEDGEMENTS

"This research has been co-financed by the European Union (European Social Fund – ESF) and Greek national funds through the Operational Program "Education and Lifelong Learning" of the National Strategic Reference Framework (NSRF) - Research Funding Program: Heracleitus II. Investing in knowledge society through the European Social Fund." The authors gratefully acknowledge this support.

REFERENCES

[1] J. Orkisz: Finite difference method (Part III). In : Handbook of Computentional Solid Mechanics. Springer, Berlin (1998) 336-432

[2] N. A. Chrysochoidis, D. A. Saravanos. High-frequency Dispertion Characteristics of Smart Delaminated Composite Beams. *Journal of Intelligent Material Systems and Structures*, 20: 1057-1068, 2009.

[3] R. Mullen, T. Belytschko. Dispertion Analysis of Finite Emenet Semidiscretizations of the Two-Dimentional Wave Equation. *International Journal of Numerical Methods in Engineering*, : 11-29, 1982.

[4] V. Vavourakis, V. I C. Protopappas, D. Fotiadis, D. Polyzos. Numerical determination of modal dispertion and AE signal characterization in waveguides though LBIE/BEM and tim-frequency analysis. *Comput Mech*, 43: 431-441, 2009.

[5] P. Kudela, M. Krawczuk, W. Ostachovic. Wave propagation in 1D structures using spectral finite elements. *Journal of Sound and Vibration*, : 88-100, 2007.

[6] J. F. Doyle. *Wave Propagation in Structures*. Springer, New York, 1997.

[7] A. T. Patera. A spectral Element Method for Fluid Dynamics: Laminar Flow in a Channel Expantion. *Journal of Computentional Physics*, : 468-488, 1984.

[8] P. Kudela, A. Zak, M. Krawczuk, W. Ostachovicz. Modelling of wave propagation in composite plates using the time domain spectral element method. *Journal of Sound and Vibration*, 302: 728-745, 2007.

[9] B. Hennings, R. Lammering. Investigation on Wave Behaviour at Defects in 2D Composite Structures Using Spectral Finite Elements in the Time Domain. 6th European Workshop on Structural Health Monitoring, Dresden, pp.269-276, 2012.

[10] Sungwon. Ha, Fu-Kuo. Chang. Optimizing a spectral element for modeling PZT-induced Lamb wave propagation in thin plates. *Smart Materials and Structures*, 19, 2010.

[11] T. S. Plagianakos, D. A. Saravanos. High-order layerwise mechanics and finite element for the damped dynamic characteristics of sandwitch composite beams. *International Journal of Solids and Structures*, : 6853-6871, 2004.

[12] K. F. Graff. *Wave Motion in Elastic Solids*. Charendon Press, Oxford, 1991.

[13] D. A. Saravanos, P. R. Heyliger. Coupled Layerwise Analysis of Composite Beams with Embedded Piezoelectrick Sensors and Actuators. *Journal of Intellgent Material Systems and Structures*, 6: 350-363, 1995.

[14] T. R. Chandrupatla, A. D. Belegundu. *Introduction to Finite Elements in Enfineering*. Prentice Hall, New Jersey, 1991.

[15] A. Zak, M. Krawczuk. Certain numerical issues of wave propagation modelling in rods by the Spectral Finite Element Method. *Finite Elements in Analysis and Design*, 47: 1036-1046, 2011.

[16] G. S. Bottai, V. Giurgiutiu. Exact Shear-Lag Solution for Guided Waves Tuning with Piezoelectric-Wafer Active Sensors. *AIAA Journal*, 50(11): 2285-2294, November 2012.

[17] K. Diamanti, C. Soutis, M. Hodgkinson. Piezoelectric transducer arrangment for the inspection of large composite structures. *Composites Part A: Applied Science and Manufacturing*, 38(4): 1121–1130, April 2007.

[18] A. Barouni, D. Saravanos. A Semi-Analytical Layerwise Solution for the Wave Propagation along a Semi-Infinite Strip with Capabilities of Damage Detection. EWSHM, Dresden, 2012.